PHYSICAL REVIEW D **89,** 054025 (2014)

Recovering the chiral critical endpoint via delocalization of quark interactions

S. Benić,[*] D. Horvatić,[†] and J. Klarić[‡]

Physics Department, Faculty of Science, University of Zagreb, Zagreb 10000, Croatia

(Received 27 January 2014; published 20 March 2014)

We show that for the lower branch of the quark condensate and values higher than approximately $-(250\ \mathrm{MeV})^3$ the chiral critical endpoint in the Nambu–Jona-Lasinio model does not occur in the phase diagram. By using lattice motivated nonlocal quark interactions, we demonstrate that the critical endpoint can be recovered. We study this behavior for a range of condensate values and find that the variation in the position of the critical endpoint is more pronounced as the condensate is increased.

DOI: 10.1103/PhysRevD.89.054025 PACS numbers: 12.39.Ki, 11.30.Rd, 12.38.Mh

I. INTRODUCTION

The possibility of a critical end point (CEP) in the QCD phase diagram is a hotly debated issue [1]. Its speculated existence bears importance for heavy ion collisions, neutron stars, and perhaps even the early Universe. Since the application of lattice QCD to high chemical potential leads to the sign problem, the answer will come from beam energy scans at RHIC, and the future NICA and FAIR facilities.

Alternatively, models can provide some guidance for arguing the location of the borders in the QCD phase diagram and in particular the existence of the CEP, see Refs. [2,3] for reviews. While in many models one finds the CEP [4–8] (for results from the Dyson-Schwinger approach, see [9,10]), functional-renormalization group studies [11], lattice calculations at imaginary chemical potential [12], interplay with superconductivity [13], or strong vector interaction [14] all point to the fact that there may be no CEP.

A simple approach to studying the chiral phase transition and its possible accompanying CEP is the Nambu–Jona-Lasinio (NJL) model [15,16]. However, even without its modifications that would include the vector channel, the diquark channel, or the Kobayashi-Maskawa-'t Hooft channel [17,18], the exact position of the CEP is rather sensitive on the value of the scalar channel coupling. In fact, as we will demonstrate, if the physical coupling is below a certain value, the CEP is not present in the phase diagram.

The intent of this work is to demonstrate that the CEP can be restored by delocalizing the interaction between quarks. In order to show this we use an instantaneous nonlocal variant of the NJL model [19–21], see also [14,22–25], allowing a smooth interpolation between highly delocalized and local NJL interactions. The idea of delocalizing quark interactions is well motivated by lattice QCD in Landau [26–28] and in Coulomb gauge [29,30] but also with Dyson-Schwinger calculations [31,32], [33] in respective gauges, where a strong infrared running of the quark propagator is observed.

We make a thorough study of the dependence of our statement on the value of the quark condensate in vacuum. Our findings demonstrate that for larger values of the condensate, the CEP is strongly increasing toward higher temperatures as the interaction is gradually delocalized. For smaller values of the condensate the dependence of the position of the CEP on the delocalization of the quark interactions is mild.

This paper is organized as follows: in Sec. II we set up the model and define its parametrizations. Section III contains our main results. In the final Sec. IV we make our conclusions.

II. MODEL

We work with the $N_f = 2$ NJL model where the delocalized 4-quark interactions are assumed to have a separable form [19–21]. The Euclidean action of the model in coordinate space is given as

$$S_E = \int d^4x \left[\bar{q}(-i\partial + m)q - \frac{G_S}{2} J_a(x) J_a(x)\right], \quad (1)$$

with currents

$$J_a(x) = \int d^4z \mathcal{F}(z) \bar{q}\left(x + \frac{z}{2}\right) \Gamma_a q\left(x - \frac{z}{2}\right), \quad (2)$$

where $\Gamma_a = (1, i\gamma_5\boldsymbol{\tau})$, $\boldsymbol{\tau}$ are Pauli matrices, G is the interaction strength and m is the current quark mass. The interaction parameter is suitably represented by a form factor $\mathcal{F}(z)$ [19]. By assuming in addition that the interaction is instantaneous, i.e., that in momentum space the form factor depends only on the square of the three-momenta $\mathcal{F}(\mathbf{p}^2)$, the thermodynamic potential in the mean-field approximation can be written as

[*] sanjinb@phy.hr
[†] davorh@phy.hr
[‡] juraklaric@gmail.com

$$\Omega = \frac{\sigma^2}{2G} - \frac{d_q}{2}\int \frac{d^3p}{(2\pi)^3}\{E + T\log[1 + e^{-\beta(E-\mu)}] + T\log[1 + e^{-\beta(E+\mu)}]\}, \quad (3)$$

where σ is the chiral mass gap, G, and $d_q = 2 \times 2 \times N_c \times N_f$. The energy of the quark quasiparticle is given as

$$E(\mathbf{p}) = \sqrt{\mathbf{p}^2 + M^2(\mathbf{p}^2)}. \quad (4)$$

Delocalization of the quark interactions has important consequence of yielding a momentum dependent quark mass $M(\mathbf{p}^2)$ which is a property seen in lattice studies, see, e.g., [29]. For the model at hand, the momentum profile is governed by the form factor

$$M(\mathbf{p}^2) = m + \sigma\mathcal{F}(\mathbf{p}^2). \quad (5)$$

The local limit is given as $\mathcal{F}(\mathbf{p}^2) = \theta(\Lambda^2 - \mathbf{p}^2)$ where Λ is the NJL cutoff. Therefore, in order to study the influence of the delocalized interactions we use a family of form factors [21]

$$\mathcal{F}(\mathbf{p}^2) = \frac{1}{1 + (\frac{\mathbf{p}}{\Lambda})^{2\alpha}}, \quad (6)$$

where $\alpha = 2$ is the smoothest form factor that can be used and still provide convergence of the gap equation, while $\alpha \to \infty$ gives the local NJL limit.

A. Parametrization

The parameters of the NJL model G, Λ and m are fixed requiring $m_\pi = 135$ MeV, $f_\pi = 92.4$ MeV and, conventionally by the vacuum value of the quark condensate[1] [21]

$$\langle\bar{q}q\rangle = -2N_c\int \frac{d^3p}{(2\pi)^3}\frac{M(\mathbf{p}) - m}{E(\mathbf{p})}. \quad (7)$$

There are two ambiguities in such a procedure. The first one is due to the fact that in the instantaneous NJL there are two values of the condensate for each coupling, known in the literature as the lower and the higher branch [21], see Fig. 1 where the condensate $\langle\bar{q}q\rangle$ is plotted as a function of the dimensionless coupling

$$g = G\Lambda^2, \quad (8)$$

by keeping $m_\pi = 135$ MeV and $f_\pi = 92.4$ MeV fixed, see Ref. [21] for the corresponding equations. The lower (higher) branch is defined by those values of g that lie on the left (right) from g that gives a minimal $\langle\bar{q}q\rangle$.

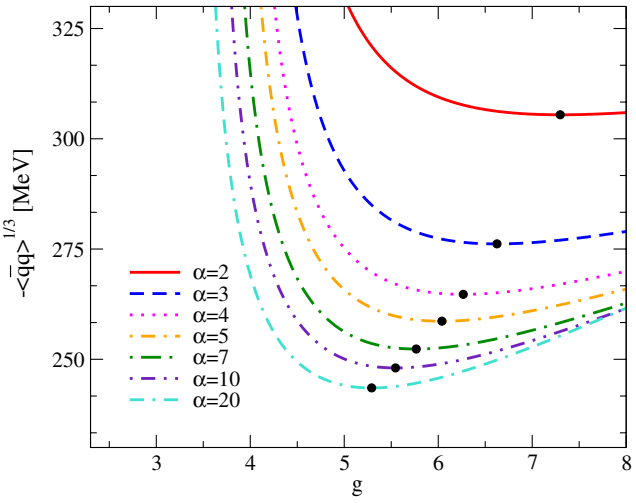

FIG. 1 (color online). We show the condensate as a function α for different reduced couplings g. Dots mark the minimal value separating the lower and the higher branch, see text.

We are interested in studying the influence of the parameter α on the CEP. The large values of g from the higher branch are not considered in this work as they yield large critical temperatures at $\mu = 0$ in comparison to $T_c(0) \simeq 170$ MeV [34] seen on the lattice. The family of parametrizations is therefore constrained on the lower branch. Notice also that in covariant nonlocal NJL models the higher branch is absent [35].

The second ambiguity comes from the value of the chosen quark condensate, which in general also depends on the renormalization scale. QCD sum rules provide a value of $-(260\text{ MeV})^3 \lesssim \langle\bar{q}q\rangle \lesssim -(190\text{ MeV})^3$ [36], and the lattice result $\langle\bar{q}q\rangle(2\text{ GeV} = -(245(4)(9)(7)\text{ MeV}$ from Ref. [37] lies within this range. Somewhat higher values are supported by recent lattice calculation: from Ref. [38] we quote $\langle\bar{q}q\rangle(2\text{ GeV} = -(265 \pm 5 \pm 22\text{ MeV})^3$, which is still within the range of sum rules, while Ref. [39] finds $\langle\bar{q}q\rangle = -(283(2)\text{ MeV})^3$. With a slight bias toward these higher values we study a range of $-(280\,\text{MeV})^3 \lesssim \langle\bar{q}q\rangle \lesssim -(240\text{ MeV})^3$.

Figure 1 shows that the condensate has a higher value as the interactions are delocalized. For example, the minimal possible value of the condensate with $\alpha = 2$ is $\langle\bar{q}q\rangle = -(305.441\text{ MeV})^3$ which is outside the said phenomenological range. Therefore, the most delocalized model that we will use is with $\alpha = 3$ where the minimal condensate is $\langle\bar{q}q\rangle = -(276.164\text{ MeV})^3$, but still keep the case $\alpha = 2$ as a curiosity.[2]

[1]Fixing the constituent quark mass $M(0)$, instead of the condensate, is another possibility [21,25] which we do not consider here.

[2]For example, by fitting the covariant nonlocal NJL model to lattice Ref. [40] obtained a rather high value of $\langle\bar{q}q\rangle = -(326\text{ MeV})^3$.

TABLE I. Family of the parameters defined by the minimal condensate for a particular value of α. The final column contains the respective critical temperatures at $\mu = 0$.

α	g	$-\langle\bar{q}q\rangle^{1/3}$ [MeV]	σ [MeV]	m [MeV]	Λ [MeV]	$T_c(0)$ [MeV]
2	7.298	305.441	610.606	2.715	511.544	251.080
3	6.625	276.165	501.450	3.660	565.332	236.659
4	6.267	264.722	467.480	4.150	579.984	232.906
5	6.039	258.636	451.596	4.447	585.127	231.582
7	5.766	252.329	436.747	4.786	587.916	230.920
10	5.545	248.038	426.880	5.037	588.235	230.700
20	5.291	243.508	419.065	5.322	586.077	231.803

The parametrization of the model is made in the following way: we start from a particular value of the condensate, which is conventionally chosen to be exactly the minimal condensate for some integer $\alpha_{\min}$. For this particular condensate we increase $\alpha > \alpha_{\min}$ along the lower branch up to the point where we reach the local limit. For practical purposes we have observed that $\alpha = 50$ is sufficient. This procedure is repeated for several values of the condensate, all conventionally being minimal for some particular integer α. A complete list of minimal values of the condensate, along with the full parametrization of the model, as well as the corresponding results for the critical temperature at zero chemical potential $T_c(0)$, is collected in Table I.

B. Critical couplings

In the limit $m = 0$ the chiral symmetry breaking in the NJL model is established only for $g > g_c$, where g_c is the critical coupling. With the delocalized interactions (6) we have

$$g_c(\alpha) = \frac{8\pi^2}{d_q}\frac{1}{1-\frac{1}{\alpha}}\frac{\sin(\pi/\alpha)}{\pi/\alpha} \tag{9}$$

showing that, for $\alpha > 2$, $g_c(\alpha)$ is necessary increasing to compensate the lack of interaction strength from delocalization. This function is represented by the dashed, black curve on Fig. 2. By increasing g beyond g_c we reach a coupling $\bar{g}_c$ where at $T = 0$ the second-order transition turns into the first order given by

$$\bar{g}_c(\alpha) = g_c(\alpha)\left[1-\left(1-\frac{1}{\alpha}\right)\frac{\sin(\pi/\alpha)}{\pi/\alpha}\left(e^{\frac{11}{6}+2\alpha}-1\right)^{-1/\alpha}\right]^{-1}. \tag{10}$$

and shown by the thick, full green line on Fig. 2. See the Appendix for the derivation of (9) and (10).

While the physical coupling always lies above g_c it does not necessary lie above $\bar{g}_c$. On Fig. 2 we show contours of physical couplings along fixed values of $\langle\bar{q}q\rangle$, f_π, and m_π, within a certain range of $\langle\bar{q}q\rangle$. Even though the physical couplings are not calculated in the chiral limit, it is indicative to observe that for higher values of the condensate, $\bar{g}_c$ crosses the physical coupling as α is increased, i.e., as we proceed to the local limit. For, e.g., the dashed, blue contour, where $\langle\bar{q}q\rangle = -(276.164\ \text{MeV})^3$ this happens around $\alpha \simeq 15$.

Furthermore, while the physical couplings at higher values of α increase at roughly the same rate as $\bar{g}_c$ by decreasing α, for smaller values of α it is not so. In fact, as the form factor gets more and more delocalized, roughly in the region $2 \lesssim \alpha \lesssim 10$, the physical coupling starts to rapidly increase. This difference between $\bar{g}_c$ and g is most severely pronounced for the somewhat unrealistic case of $\langle\bar{q}q\rangle = -(305.441\ \text{MeV})^3$, where Fig. 2 shows that $\bar{g}_c$ even drops a bit at $\alpha = 2$.

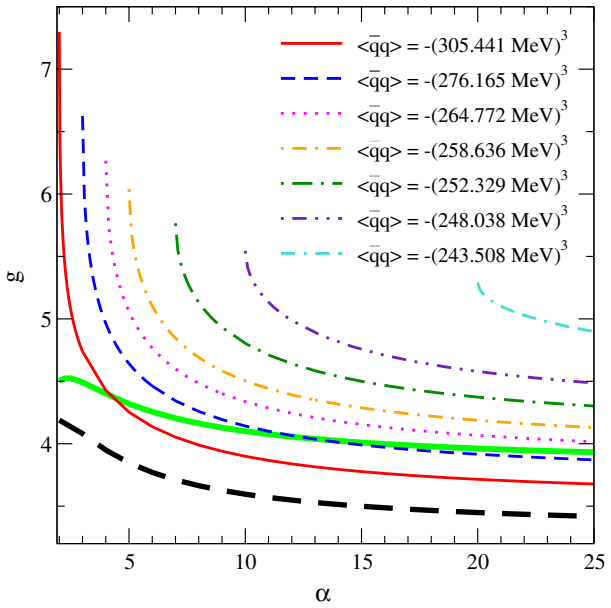

FIG. 2 (color online). We display contours of physical values of coupling g as functions of α, indicating the particular values of the condensate used. Note that every point on these curves represents a particular parametrization of the instantaneous NJL model. The variation of the critical couplings (dashed, black line) for chiral symmetry breaking, and for first order transition (full, light green line), g_c and $\bar{g}_c$, respectively, is also shown.

III. PHASE DIAGRAM AND THE CRITICAL END POINT

In this section we study the variation in the position of the chiral CEP by tuning the nonlocality parameter α. We are particularly interested in what happens for very small values of α. First we find the phase diagram in the chiral limit, for several values of α. For physical current mass, and for several values of $\langle\bar{q}q\rangle$, we employ the parametrization stated in the previous section and calculate the CEP for a range of α.

In order to calculate the phase diagram and the CEP we first solve the gap equation

$$\frac{\partial\Omega}{\partial\sigma} = 0, \tag{11}$$

and find all possible solutions. In the case of the second-order phase transition (crossover) there is always one stable and one unstable solution. The chiral transition line is found numerically from the divergence (peak) of the thermal susceptibility $d\sigma/dT$ for the stable solution. In the case of the first-order phase transition there are two stable and one unstable solutions, so the chiral transition is defined by identifying the global stable solution. Finally, the CEP is calculated as the point where the unstable solution observed in the first order region merges with the remaining stable solutions.

A. Chiral limit

In the chiral limit we provide a clean example of the impact of the crossing of $\bar{g}_c$ and the physical coupling. For that purpose we set up a special parametrization where the physical coupling in the limit $\alpha \to \infty$ is exactly equal to $\bar{g}_c$ (10). This means that in the local NJL limit and the chiral limit, the critical endpoint lies exactly at $T = 0$ given by

$$\mu_c = \Lambda\sqrt{1 - \frac{g_c}{g}}, \tag{12}$$

when $g \to \bar{g}_c$ in the NJL limit, see Appendix A. The parametrizations of the model are performed for physical quark masses, but the calculation of the phase diagram will be performed in the chiral limit. The condensate which satisfies the previously stated requirements is $\langle\bar{q}q\rangle = -(265.573\ \text{MeV})^3$. We then decrease α towards the smoothest possible form factor allowed by this particular value of $\langle\bar{q}q\rangle$, which turns out to be $\alpha = 4$. The relevant results of this particular parametrization procedure are collected in Table II.

The chiral transition lines in the limit $m = 0$ are shown in the $\mu - T$ plane in Fig. 3 for several values of α. Due to our choice of the physical coupling, the phase diagram for $\alpha = 50$ has a CEP exactly on $T = 0$. Therefore, $\alpha = 50$ is an excellent approximation of the local model. The effect of delocalizing the quark interactions is that the CEP increases significantly toward nonzero temperatures, while the chemical potential of the CEP does not change much. For the smallest α possible, $\alpha = 4$, the CEP has a temperature of about $T \simeq 125$ MeV.

TABLE II. Family of the parameters for $\langle\bar{q}q\rangle = -(265.573\ \text{MeV})^3$.

α	g	σ [MeV]	m [MeV]	Λ [MeV]
4	5.799	412.066	4.111	603.352
5	5.011	328.943	4.113	662.998
20	4.053	261.009	4.116	746.387
50	3.903	254.578	4.117	755.169

Our results are roughly in accordance with the ones shown on Fig. 2. The physical coupling given by the dotted, magenta line has almost the same $\langle\bar{q}q\rangle$ as used here, and approaches $\bar{g}_c$, given by the full, green line, for large values of α. By contrast, decreasing α leads to a large mismatch between the physical coupling and $\bar{g}_c$, allowing the CEP to significantly increase in the temperature.

The increase in the critical temperature and the chemical potential as α is lowered is in part due to the increase in the difference between g and $\bar{g}_c$, see Fig. 2 but also because the scale Λ is increasing, see Table II.

B. Physical quark masses

At physical quark masses we calculate the CEP for values of $\langle\bar{q}q\rangle$ defined in Sec. II B. Our main result is shown in Fig. 4 where location of the CEP, corresponding

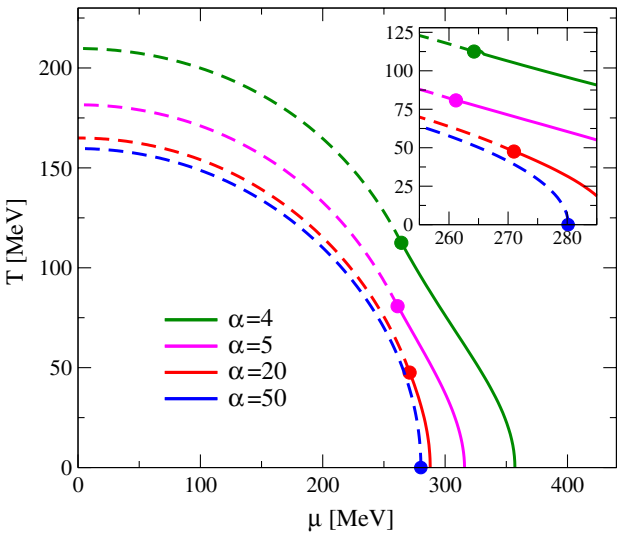

FIG. 3 (color online). The figure shows several chiral transition curves in the limit $m = 0$ for $\langle\bar{q}q\rangle = -(265.573\ \text{MeV})^3$. We use the parameter sets from Table II where we put $m = 0$ by hand. The dashed (full) lines are the second (first) order phase transition. The case $\alpha = 50$, where the CEP is located at $T = 0$, is effectively the local NJL limit.

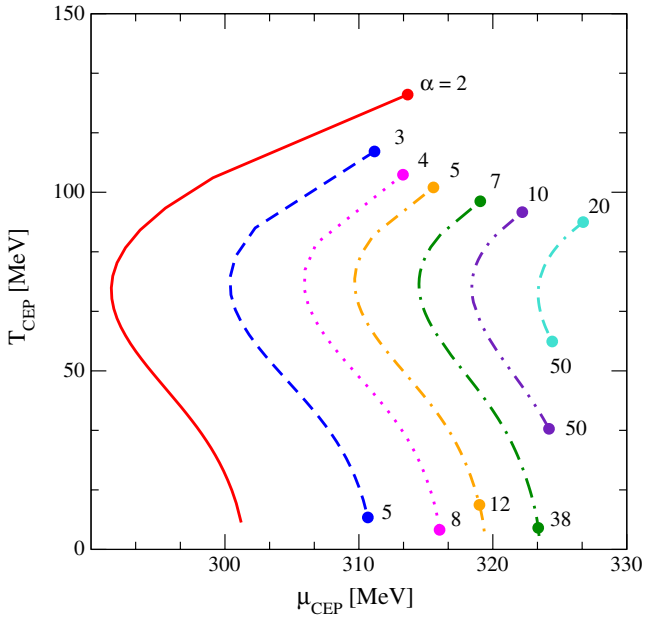

FIG. 4 (color online). Each curve denotes the position of the CEP as a function of α, for a particular value of the $\langle\bar{q}q\rangle$. We use the same values of $\langle\bar{q}q\rangle$ and the same line styles as defined in Fig. 2. The values of $\langle\bar{q}q\rangle$ are decreased in magnitude as we proceed from the left-most to the right-most curve. The upper dots indicate the value of the CEP for minimal values of the condensate, see Table I. The parameter α is varied continuously. The lower dots indicate the last integer value of α where the CEP occurs in the phase diagram.

to these values of $\langle\bar{q}q\rangle$, of the CEP is shown as a function of α, where, starting from the its minimal value α is varied continuously. We observe that for several higher values of $\langle\bar{q}q\rangle$, up to roughly $\langle\bar{q}q\rangle \simeq -(250\ \mathrm{MeV})^3$, the CEP vanishes from the phase diagram as α is increased. Only by delocalizing the quark interactions are we able to recover CEP in the phase diagram.

Physically, this effect is due to the following. The crossing of the physical coupling and $\bar{g}_c$ at large α expels the CEP from the phase diagram, while the large mismatch at low α is responsible for shifting the CEP to high T.

For high values of the condensate, such as that shown by the dashed, blue line, only the very delocalized interactions are able to hold the CEP in the phase diagram. Namely, the CEP proceeds rapidly from $T \simeq 100$ MeV at $\alpha = 3$ to $T \simeq 0$ MeV already for any $\alpha > 5$. It is interesting to observe that the CEP does not proceed to $T = 0$ by reducing both T and μ. Rather, this happens only for the first few values of α, whereas for higher α only T is decreased, while μ increases. This effect is also seen in the chiral limit, see the inset of Fig. 3.

In the opposite case, when there is no crossing and the physical coupling changes at a similar rate as $\bar{g}_c$, the CEP is effectively immobilized. In particular, already for the values of $\langle\bar{q}q\rangle = -(243.508\ \mathrm{MeV})^3$ shown on Fig. 4, the right-most, cyan line gives a variation of $\sim$30 MeV in the temperature. In such a scenario the CEP is always present. This is to be expected from the results obtained in the previous section, and shown in Fig. 2, where low values of $\langle\bar{q}q\rangle$ do not allow small α and thus the physical coupling always lies above $\bar{g}_c$. Since the actual contours of g shown in Fig. 4 are for physical quark masses, while $\bar{g}_c$ is obtained in the chiral limit, the values of α at which no CEP occurs in the phase diagram is a bit higher than the values of α at which the curves in Fig. 2 cross $\bar{g}_c$.

Finally, observe that for $\langle\bar{q}q\rangle = -(305.441\ \mathrm{MeV})^3$, already with $\alpha = 3$ no CEP occurs in the phase diagram. The slight offset from the starting points of the other families of curves is attributed to a slight reduction of $\bar{g}_c$ at $\alpha = 2$.

IV. CONCLUSIONS

In this work we have examined how the delocalization of the quark interactions within the framework of the instantaneous Nambu–Jona-Lasinio model influences the position of the CEP in the phase diagram. Motivated by the lattice calculations [29] where the quark dressing functions, and in particular the mass function, smoothly changes with momentum we find that the very smooth form factors in the instantaneous NJL model are possible for the values of the condensate around $\langle\bar{q}q\rangle \simeq -(280\ \mathrm{MeV})^3$. This is somewhat higher than the typical values quoted from the sum rules [36], but interestingly, close to a recent prediction from the lattice [39].

We show that delocalization of the quark interactions drastically influences the position of the CEP. In particular, there is a gap in the temperature of $T \sim 100$ MeV between the results in the nonlocal model with respect to the ones in the local model where the CEP tends to disappear from the phase diagram. The minimal value for which this happens, given roughly as $\langle\bar{q}q\rangle \simeq -(250\ \mathrm{MeV})^3$ is still within the range of the values reported from sum rules. For all higher values the temperature gap is rather robust to the increase of $\langle\bar{q}q\rangle$. Lowering the condensate restricts us to using only rather local form factors which in turn immobilize the CEP and still keep it in the in the phase diagram.

It would be interesting to test further the implications of the nonlocal interactions on the CEP when the full structure of the quark propagator, with the wave function renormalization channel taken into account.

ACKNOWLEDGMENTS

We would like to thank D. Blaschke and H. Grigorian for useful discussions. S. B. acknowledges the kind hospitality at the Mini-Symposium on "Dynamics of Correlations in Dense Hadronic Matter" in Wrocław. S. B. and D. H. received support by the University in Zagreb under Contract No. 202348. This work was supported in part by the COST Action MP1304 "NewCompStar".

APPENDIX: CRITICAL COUPLING FOR FIRST-ORDER PHASE TRANSITION

In order to find the critical coupling for which the CEP in the limit $m = 0$ lies exactly at $T = 0$, we make a Landau expansion of the thermodynamic potential

$$\Omega = \Omega|_{\sigma=0} + \left.\frac{\partial^2\Omega}{\partial\sigma^2}\right|_{\sigma=0}\sigma^2 + \left.\frac{\partial^4\Omega}{\partial\sigma^4}\right|_{\sigma=0}\sigma^4 + \cdots, \tag{A1}$$

where

$$\begin{aligned}\left.\frac{\partial^2\Omega}{\partial\sigma^2}\right|_{\sigma=0} &= \frac{\Lambda^2}{g} - \frac{d_q}{2}\int\frac{d^3p}{(2\pi)^3}\frac{\mathcal{F}^2(\mathbf{p}^2)}{|\mathbf{p}|}(1-\theta(\mu-|\mathbf{p}|)) \\ &= \frac{\Lambda^2}{g} - \frac{\Lambda^2}{g_c} - \frac{d_q}{16\pi^2}\frac{\mu^2}{\alpha}\left[\mathcal{F}(\mu^2) + (\alpha-1)_2F_1\left(1,\frac{1}{\alpha},1+\frac{1}{\alpha};-\left(\frac{\mu}{\Lambda}\right)^{2\alpha}\right)\right],\end{aligned} \tag{A2}$$

$$\begin{aligned}\left.\frac{\partial^4\Omega}{\partial\sigma^4}\right|_{\sigma=0} &= \frac{3d_q}{2}\int\frac{d^3p}{(2\pi)^3}\left[\frac{\mathcal{F}^4(\mathbf{p}^2)}{|\mathbf{p}|^3}(1-\theta(\mu-|\mathbf{p}|)) + \frac{\mathcal{F}^4(\mathbf{p}^2)}{\mathbf{p}^2}\delta(\mu-|\mathbf{p}|)\right] \\ &= -\frac{3d_q}{4\pi^2}\left\{\mathcal{F}^4(\mu^2) + \frac{1}{6\alpha}\mathcal{F}^3(\mu^2) + \frac{1}{4\alpha}\mathcal{F}^2(\mu^2) + \frac{1}{2\alpha}\mathcal{F}(\mu^2) + \frac{1}{2\alpha}\log\left[\left(\frac{\mu}{\Lambda}\right)^{2\alpha}\mathcal{F}(\mu^2)\right]\right\}.\end{aligned} \tag{A3}$$

The function $\mathcal{F}(\mathbf{p}^2)$ is defined in Eq. (6) and ${}_2F_1(a,b,c;x)$ is the hypergeometric function. Requiring that both (A2) and (A3) vanish we find two equations for g and μ defining the CEP. By assuming $\mu \ll \Lambda$ these yield the critical chemical potential

$$\mu_c = \frac{\Lambda}{(e^{\frac{11}{6}+2\alpha}-1)^{1/2\alpha}}, \tag{A4}$$

and the critical coupling

$$\bar{g}_c(\alpha) = g_c(\alpha)\left[1 - \left(1-\frac{1}{\alpha}\right)\frac{\sin(\pi/\alpha)}{\pi/\alpha}(e^{\frac{11}{6}+2\alpha}-1)^{-1/\alpha}\right]^{-1}. \tag{A5}$$

In the limit $\alpha \to \infty$ they are given as

$$\mu_c = \frac{\Lambda}{e}, \tag{A6}$$

and

$$\bar{g}_c = \frac{g_c}{1-e^{-2}}, \tag{A7}$$

respectively.

[1] M. A. Stephanov, *Proc. Sci.*, LAT2006 (**2006**) 024.
[2] K. Fukushima and T. Hatsuda, Rep. Prog. Phys. **74**, 014001 (2011).
[3] K. Fukushima and C. Sasaki, Prog. Part. Nucl. Phys. **72**, 99 (2013).
[4] D. Gomez Dumm, D. B. Blaschke, A. G. Grunfeld, and N. N. Scoccola, Phys. Rev. D **73**, 114019 (2006).
[5] K. Fukushima, Phys. Rev. D **77**, 114028 (2008); **78**039902 (E) (2008).
[6] T. Hell, S. Roessner, M. Cristoforetti, and W. Weise, Phys. Rev. D **79**, 014022 (2009).
[7] G. A. Contrera, M. Orsaria, and N. N. Scoccola, Phys. Rev. D **82**, 054026 (2010).
[8] G. A. Contrera, A. G. Grunfeld, and D. B. Blaschke, arXiv:1207.4890 [Phys. Part. Nucl. Lett. (to be published)].
[9] C. S. Fischer and J. A. Mueller, Phys. Rev. D **80**, 074029 (2009).
[10] S.-x. Qin, L. Chang, H. Chen, Y.-x. Liu, and C. D. Roberts, Phys. Rev. Lett. **106**, 172301 (2011).

[11] T. K. Herbst, J. M. Pawlowski, and B.-J. Schaefer, Phys. Lett. B **696**, 58 (2011).
[12] P. de Forcrand and O. Philipsen, J. High Energy Phys. 01 (2007) 077.
[13] T. Hatsuda, M. Tachibana, N. Yamamoto, and G. Baym, Phys. Rev. Lett. **97**, 122001 (2006).
[14] C. Sasaki, B. Friman, and K. Redlich, Phys. Rev. D **75**, 074013 (2007).
[15] Y. Nambu and G. Jona-Lasinio, Phys. Rev. **122**, 345 (1961).
[16] Y. Nambu and G. Jona-Lasinio, Phys. Rev. **124**, 246 (1961).
[17] U. Vogl and W. Weise, Prog. Part. Nucl. Phys. **27**, 195 (1991).
[18] M. Buballa, Phys. Rep. **407**, 205 (2005).
[19] S. M. Schmidt, D. Blaschke, and Y. L. Kalinovsky, Phys. Rev. C **50**, 435 (1994).
[20] D. Blaschke, Y. L. Kalinovsky, L. Munchow, V. N. Pervushin, G. Ropke, and S. M. Schmidt, Nucl. Phys. **A586**, 711 (1995).
[21] H. Grigorian, Phys. Part. Nucl. Lett. **4**, 223 (2007).
[22] D. Blaschke, Y. L. Kalinovsky, G. Roepke, S. M. Schmidt, and M. K. Volkov, Phys. Rev. C **53**, 2394 (1996).
[23] D. Blaschke, S. Fredriksson, H. Grigorian, and A. M. Oztas, Nucl. Phys. **A736**, 203 (2004).
[24] H. Grigorian, D. Blaschke, and D. N. Aguilera, Phys. Rev. C **69**, 065802 (2004).
[25] D. N. Aguilera, D. Blaschke, H. Grigorian, and N. N. Scoccola, Phys. Rev. D **74**, 114005 (2006).
[26] M. B. Parappilly, P. O. Bowman, U. M. Heller, D. B. Leinweber, A. G. Williams, and J. B. Zhang, Phys. Rev. D **73**, 054504 (2006).
[27] W. Kamleh, P. O. Bowman, D. B. Leinweber, A. G. Williams, and J. Zhang, Phys. Rev. D **76**, 094501 (2007).
[28] M. Schrock, Phys. Lett. B **711**, 217 (2012).
[29] G. Burgio, M. Schrock, H. Reinhardt, and M. Quandt, Phys. Rev. D **86**, 014506 (2012).
[30] G. Burgio, M. Quandt, H. Reinhardt, and M. Schrock, *Proc. Sci*, ConfinementX (**2012**) 075 [arXiv:1301.3619].
[31] C. S. Fischer, J. Phys. G **32**, R253 (2006).
[32] C. D. Roberts, arXiv:1203.5341.
[33] M. Pak and H. Reinhardt, Phys. Lett. B **707**, 566 (2012).
[34] S. Ejiri, Nucl. Phys. B, Proc. Suppl. **94**, 19 (2001).
[35] D. Gomez Dumm, A. G. Grunfeld, and N. N. Scoccola, Phys. Rev. D **74** (2006) 054026.
[36] H. G. Dosch and S. Narison, Phys. Lett. B **417**, 173 (1998).
[37] L. Giusti, F. Rapuano, M. Talevi, and A. Vladikas, Nucl. Phys. **B538**, 249 (1999).
[38] V. Gimenez, V. Lubicz, F. Mescia, V. Porretti, and J. Reyes, Eur. Phys. J. C **41**, 535 (2005).
[39] C. McNeile, A. Bazavov, C. T. H. Davies, R. J. Dowdall, K. Hornbostel, G. P. Lepage, and H. D. Trottier, Phys. Rev. D **87**, 034503 (2013).
[40] S. Noguera and N. N. Scoccola, Phys. Rev. D **78**, 114002 (2008).